Journal of Structural Chemistry. Vol. 58, No. 6, pp. 1069-1078, 2017.

PHOTOELECTRON SPECTRA AND ELECTRONIC STRUCTURE OF NITROGEN-CONTAINING CHELATE BORON COMPLEXES

S. A. Tikhonov, I. B. Lvov, and V. I. Vovna* UDC 544.15:544.17:544.18

A brief review of the results of studying some classes of nitrogen-containing chelate boron complexes by ultraviolet photoelectron spectroscopy and density functional theory is reported. The quantum chemical modeling of the substitution effects of a complexing agent, heteroatoms, and functional groups in α, β, and γ positions of the chelate ring allowed us to establish the features of the electronic structure of the studied complexes. It is found that the substitution of heteroatoms in the chelate ring has no substantial influence on the structure of the highest occupied molecular orbital (HOMO). In imidoylamidinate complexes, as opposed to formazanates and β-diketonates, there is no noticeable mixing of π orbitals of the chelate and benzene rings. In condensed nitrogen heterocycles the HOMO is stabilized by 0.2-0.3 eV and π orbitals of the benzene ring are stabilized by 0.8-1.2 eV. The HOMO of substituted aza-boron-dipyridomethene correlates with anthracene and acridine π_7 orbitals, which causes the fine structure of the first band. It is shown that in an energy range below 11 eV the calculated results reproduce well the energy gaps between the ionization states of the complexes.

DOI: 10.1134/S0022476617060038

Keywords: electronic structure, photoelectron spectroscopy, density functional theory, boron chelates, β-diketonates, imidoylamidinates, formazanates.

INTRODUCTION

The luminescent properties and the relatively easy preparation of chelate boron complexes determine the promising use of materials based on them. In particular, boron β-diketonates ($X_2B(O–C(R_1)–C(R_2)–C(R_3)–O$) exhibit intensive luminescence [1-5], liquid crystalline properties [6-8], high biological activity [9] and find their application as laser dyes [10], active components of solar collectors [11], materials for nonlinear optics [12], polymeric optical materials [13, 14] and antivirals [9]. No less relevant are the investigations of the optical properties of nitrogen-containing analogues of boron β-diketonates. The luminescent properties of boron imidoylamidinates ($X_2B(NH–C(R_1)–N–C(R_2)–NH$) and boron formazanates ($X_2B(N(R_1)–N–C–N–N(R_2)$ determine their possible application as laser dyes [15-19]. A set of specific properties [20, 21] of boron dipyrido methylene (BODIPY) and its derivatives determine the prospects of using BODIPY-based materials as active components of solar collectors [22], biomolecular markers [23], and optical chemosensors [24].

Far Eastern Federal University, Vladivostok, Russia; *vovna.vi@dvfu.ru. Translated from *Zhurnal Strukturnoi Khimii*, Vol. 58, No. 6, pp. 1115-1124, July-August, 2017. Original article submitted December 26, 2016; revised January 10, 2017.

The establishment of relationships between the functional characteristics of the substances and their electronic structures opens the ways for the synthesis of novel compounds with the desired properties. The most reliable information on the electronic structure of the complexes can be obtained by a combined application of ultraviolet photoelectron spectroscopy (UPS) and quantum chemistry methods. UPS is a direct method to examine the electronic structure of valence and core levels [25]. The direct UPS measurement of the characteristics of individual levels enables a comparison of the obtained results with the calculated electron energies. Good correlation between the experimental and theoretical energies evidences the validity of the modeling results. As we have shown in [26], the calculations at the density functional theory (DFT) level allow the estimation of ionization energies (IEs) of the boron complexes with an accuracy of 0.1 eV.

Previously, we have reported the results of the UPS and DFT investigation of the electronic structure of boron β-diketonates [27-31] and their nitrogen-containing analogues [32-34]. To examine the electronic effects of heteroatom substitution in the chelate ring, we analyzed the information on the electronic structures of the model compounds: β-diketonate (**I**), imidoylamidinate (**II**), and formazanate (**III**) complexes. The regularities found were used in the analysis of the UPS data and DFT calculations of boron imidoylamidinates and formazanates containing different organic substituents in α, β, and γ positions of the chelate ring and the boron atom.

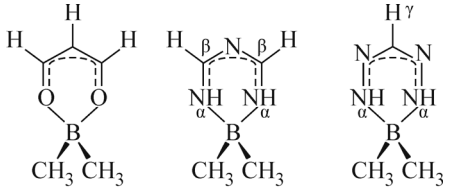

Scheme 1. Compounds **I–III**.

EXPERIMENTAL AND COMPUTATIONAL TECHNIQUES

The samples of the chelate complexes were synthesized at the Zelinsky Institute of Organic Chemistry, Russian Academy of Sciences, according to the procedures described in [35-37]. The UPS spectra of vapor of compounds **IV–XVIII** (Schemes 2-4) were recorded on a modified ES-3201 electron spectrometer with a monochromatic He I radiation source ($h\nu$ = 21.2 eV). A determination error of the band peaks did not exceed 0.08 eV. The temperature of an ionization cuvette depended on the vapor sublimation temperature of a certain sample and varied from 180 °C to 240 °C. All UPS spectra have bands in an energy range from 7 eV to 11 eV.

The UPS spectral bands were compared with the calculated energies with regard to the number of theoretical electronic levels, energy gaps between them, and the ionization cross-sections. The computational technique was chosen due to good correlation between the experimental and theoretical ionization energies of the chelate boron complexes [26]. This is explained by the similarity of the Kohn–Sham equation and the quasi-particle Dyson equation. The general Dyson equation [38] is one of the ways to derive the Green functions [39]. In [40, 41], it was shown that Kohn–Sham orbitals could serve as a good approximation to Dyson orbitals in the valence band.

The electronic structures of compounds **I–XVIII** (Schemes 1-4) were calculated using the Firefly 8.1.G software [42] with the TZVPP basis set [43, 44]. For the quantum chemical calculations of the boron complexes [45-48] the hybrid three-parameter B3LYP functional has been successfully applied [49-51]. In this work and in [26-34] we performed the calculations using the B3LYP functional. This enabled us to exclude the influence of the functional on the electronic substitution effects.

In the comparison of the experimental ionization energies (IE_i) with calculated electron energies ε_i the procedure analogous to the Koopmans theorem ($IE_i = -\varepsilon_i + \delta_i$) was used, where δ_i is the correction for the orbital energy of the *i* level (DFA defect).

The UPS spectral bands corresponding to several orbitals were fitted with Gaussians. In the Gaussian fitting of the spectral bands, the number of calculated electronic levels, energy gaps between them, and the similarity in the ionization cross-sections were taken into account. The Gaussian peak energies IE_g were taken for IE_i values.

In the text and tables, the preferred localization of molecular orbitals (MOs) is denoted by the following indices: X for the localization on the complexing agent $(C_3H_7)_2B$, $(C_4H_9)_2B$, $(C_6H_5)_2B$, Ac_2B; R for the localization on the substituents in α, β, and γ positions of the chelate ring (C_2H_5, C_6H_5, H, 2-$C_6H_4CH_3$, 4-$C_6H_4CH_3$, cyclohexyl, cyclohexylamine). The notation n_N is used for the σ type orbitals localized more on nitrogen atoms (lone pair).

RESULTS AND DISCUSSION

β-Diketonate, imidoylamidinate, and formazanate complexes (model compounds). Fig. 1 depicts the chart of calculated energies of three isoelectronic analogues: β-diketonate (**I**), imidoylamidinate (**II**), and formazanate complex (**III**). The symmetry group of these compounds is C_{2v}.

The mixing of π_3 orbitals of the chelate ring and the complexing agent X is observed for the HOMOs of compounds **I–III** (Figs. 1, 2). The energy gap between the π_3–X and X+π_3 levels is 1.67 eV (**I**), 2.05 eV (**II**), and 2.25 eV (**III**). A large splitting of the π_3 level in nitrogen-containing compounds **II** and **III** is due to the effect of nitrogen *n* orbitals (Figs. 1 and 2). The HOMO-1 of complex **II** is localized more on the nitrogen atom in the γ position, which is explained by the presence of a lone pair. The HOMO-1 of compound **III** is localized on four nitrogen atoms. In complexes **II** and **III**, the n_+ orbital mixes with the X orbital. The energy gap between the π_3–X and n_- levels is 0.47 eV and 1.10 eV for compounds **I** and **III**.

Six-membered complexes. In this section the results of the analysis of the electronic structures of compounds **IV–VII** are discussed [32, 34].

According to the calculated data, the molecules of **IV–VI** have symmetry group C_2. The structure of compound **VII** is close to symmetry group C_2. The minimum total energy of compounds **IV–V** is observed when the C_2H_5 fragments of the propyl groups of the complexing agent are located on either side of the plane perpendicular to the chelate ring. The phenyl

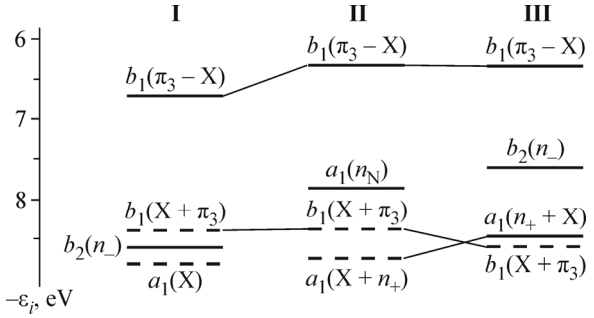

Fig. 1. Correlation chart of four higher occupied π and σ MOs of compounds **I–III**. The preferred MO localization is denoted by: bold line for the chelate ring, dashed line for the complexing agent X.

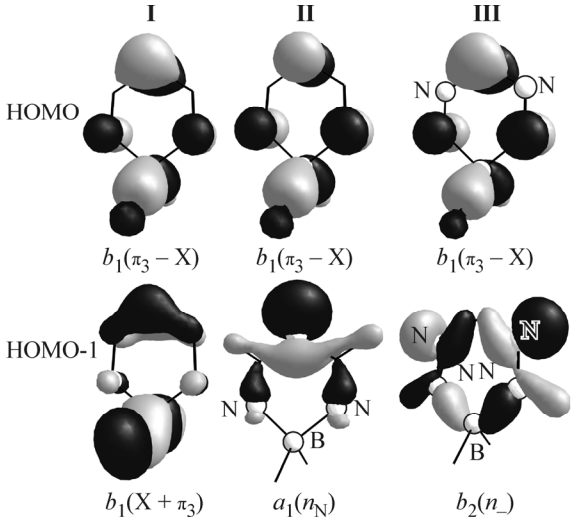

Fig. 2. Shapes of the HOMO and HOMO-1 of the model compounds.

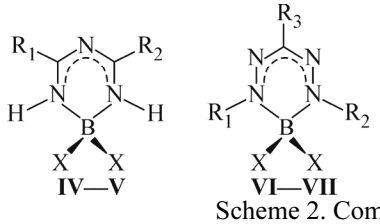

IV $R_1=R_2=Et$
V $R_1=R_2=Ph$
VI X=Ac, $R_1=R_2=Ph$, $R_3=H$
VII X=Ac, $R_1=R_2=Ph$, R_3=4-toluyl

Scheme 2. Compounds **IV–VII**.

group substitution for ethyl groups at the carbonyl carbon atoms (complex **V**) does not noticeably change the bond lengths in the chelate ring, and the dihedral angles between the planes of the chelate and benzene rings are 25°. For complexes **VI** and **VII** the violation of complanarity of the planes of the chelate and benzene rings is also observed; the corresponding dihedral angle is 47°. In compound **VII**, the chelate ring and the $C_6H_4CH_3$ substituent are in one plane.

The analysis of the results of the electronic structure modeling for complexes **IV–V** showed the mixing of the π_3 orbitals of the chelate ring with MOs of complexing agent X (Table 1, Fig. 3). There is no noticeable mixing of π_3 and R MOs in compound **V** (Table 1, Fig. 3). The presence of four orbitals of benzene rings does not cause a noticeable change in the energy gap between the π_3–X and X+π_3 levels as compared to model compound **II** (Fig. 1, Table 1).

For **VI** and **VII**, as opposed to **V**, a noticeable mixing of π orbitals of the chelate and benzene rings (Table 1, Fig. 3) is observed, which is typical of boron β-diketonates [27, 29, 31]. The orbital mixing results in stabilizing the HOMO of complex **VI** by 0.50 eV relative to **V** (Table 1). The presence of the $C_6H_4CH_3$ group as a substituent (complex **VII**) leads to noticeable MO delocalization. In compound **VII**, the π_3 orbital of the chelate ring mixes with the π_3 MO of toluyl resulting in the destabilization of HOMO electron energies by 0.53 eV as compared to compound **VI** (Fig. 3, Table 1). Due to the effect of additional π MOs of the $C_6H_4CH_3$ substituent the splitting of the π_3 level increases by 0.69 eV.

The UPS spectra of compounds **V–VII** (bold lines) whose bands are fitted with Gaussians (thin lines) are depicted in Fig. 4. In the Gaussian fitting of the spectral bands, the number of calculated electronic levels, energy gaps between them, and the similarity of the ionization cross-sections were taken into account. The vertical lines in the spectra correspond to the calculated electron energies shifted by a value of the DFA defect. To demonstrate good correlation of the UPS data with the modeling results, Fig. 4 presents the theoretical spectra of compounds **V–VII** (gray lines). The relative cross- sections of the components (asymmetry parameter of 1.10) of the DFT spectra with the prevailing contribution of oxygen and nitrogen AOs is smaller than the corresponding values for carbon orbitals by 20%. The half-height width of all DFT spectral components is 0.50.

By analogy with boron β-diketonate complexes [27-31], in the spectra of compounds **V–VII** the bands corresponding to the HOMOs are broad (Fig. 4). The shape of the first band in the UPS spectra of compounds **V–VII** is determined by a set of components for 3*N*-6 vibrations. Following the Franck–Condon principle, substantial changes in the

TABLE 1. Orbital Electron Energies (eV) and the Positions of Band Peaks from the Results of Gaussian Fitting of the Experimental Spectra (eV) of Compounds **IV–VII**

Compound	MO	π_3–X	R–π_3	R–X	R	X–R	n_-+X	R+π_3	n_N	X+π_3	X+n_N
IV	$-\varepsilon_i$	5.76	–	–	–	–	–	–	7.34	7.57	7.72
	IE_i	7.75	–	–	–	–	–	–	9.41	9.66	9.87
V	$-\varepsilon_i$	5.83	–	–	7.09-7.33	–	–	–	7.57	7.79	7.81
	IE_i	7.59	–	–	8.86-9.23	–	–	–	9.44	9.56	9.67
VI	$-\varepsilon_i$	–	6.33	6.97; 7.05	7.22	7.33; 7.42	7.53	8.06	–	–	–
	IE_i	–	8.32	9.07; 9.33	9.37	9.47; 9.70	9.78	10.12	–	–	–
VII	$-\varepsilon_i$	–	5.79	6.91; 7.05	6.99-7.22	7.34; 7.42	7.45	8.20	–	–	–
	IE_i	–	7.84	9.20; 9.30	9.30-9.58	9.70; 9.80	9.85	10.40	–	–	–

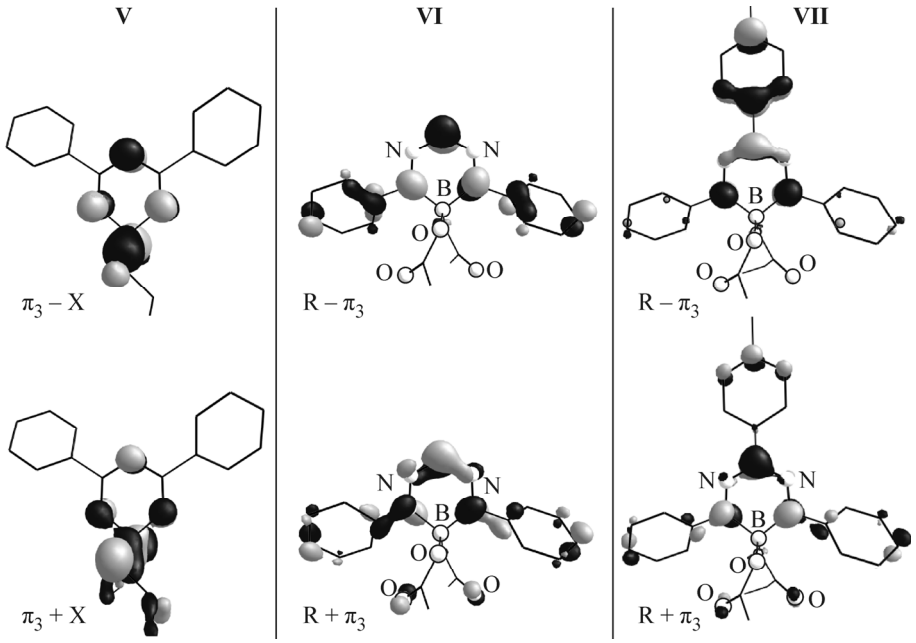

Fig. 3. Shape of some MOs of compounds **V–VII**.

equilibrium coordinates of stretching and bending vibrations in the ion, cause a 0.58-0.87 eV excess in the vertical transition energy as compared to the adiabatic transition. The maximum width of the first band is observed for the spectrum of **VI**, which is explained by the HOMO delocalization on three rings (Fig. 3).

The shapes of Gaussian components in the spectra of compounds **V–VII** are asymmetric (Fig. 4), which is also typical of π and *n* MOs of benzene molecules [52], heterocycles [53], boron β-diketonate complexes [27-31], and their nitrogen analogues. The asymmetry parameter of the first band (the right/left half-width ratio) for compounds **V** and **VII** is, respectively, 1.12 and 1.10. The first and second spectral bands are observed to overlap for substance **VI**, which hinders the determination of the asymmetry parameter. According to the results of the fitting, the first band in the spectrum of compound **VI** is symmetrical.

Boron imidoylamidinates with condensed rings. Below, the results of the analysis of the electronic structures of compounds **VIII–XV** are reported [32, 33].

In a series of compounds **VIII–XV** an insignificant violation of complanarity of the planes of condensed rings is observed. By analogy with complexes **V–VI**, in **IX–XI** and **XIII–XV** the violation of complanarity of the chelate ligand and substituent planes occurs. The respective dihedral angles range from 22° to 38°.

The calculation of compounds **VIII–XV** showed a significant mixing of orbitals of the chelate ligand and the complexing agent (Table 2), which is observed for boron acetylacetonates with organic substituents [30]. Five higher occupied MOs of complexes **VIII–X** are of similar character. *Ortho*-position methylation of the phenyl ring (compound **XI**) noticeably changes the character and energy of the fourth, fifth, and sixth higher MOs.

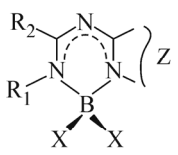

VIII X=Pr, Z= =N–CH=N–, R_1=R_2=H
IX X=Pr, Z= =N–CH=N–, R_1=H, R_2=Ph
X X=Pr, Z= =N–CH=N–, R_1=H, R_2=4-toluyl
XI X=Pr, Z= –N–CH=N–, R_1=H, R_2=2-toluyl
XII X=Bu, Z= –S–CH=CH–, R_1=R_2=H
XIII X=Bu, Z= –S–CH=CH–, R_1=H, R_2=4-toluyl
XIV X=Pr, Z= –S–CH=CH–, R_1=cyclohexyl, R_2=cyclohexylamine
XV X=Pr, Z= –N–CH=CH–, R_1=cyclohexyl, R_2=cyclohexylamine

Scheme 3. Compounds **VIII–XV**.

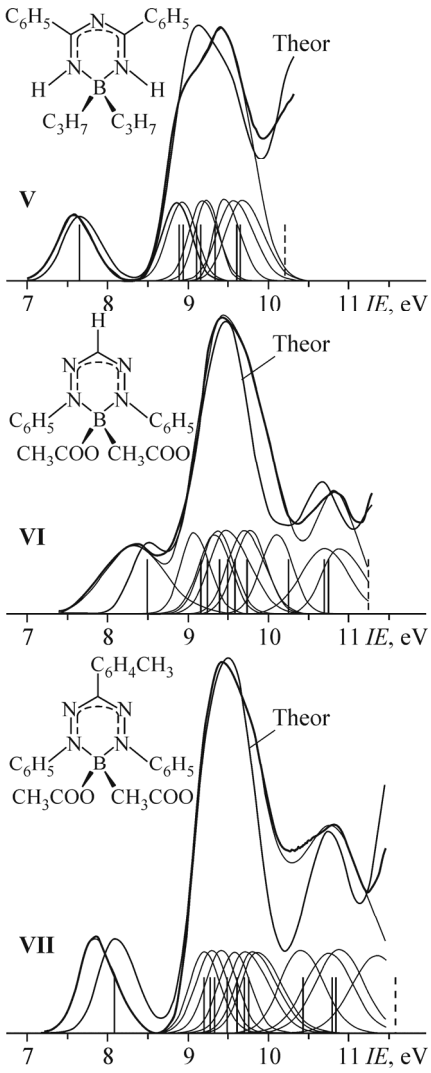

Fig. 4. UPS spectra of vapor of compounds **V–VII** [34].

In complexes **IX–XI** and **XIII**, by analogy with **V**, there is no noticeable mixing of π orbitals of the ligand and the benzene ring (Table 2). In a series of compounds **IX–XI** the MO electronic levels of substituent R are by 0.6-1.0 eV lower than the respective levels in complex **V** (Tables 1 and 2). This is caused by the field effect of the six-membered ring, which donated the electron density to the five-membered ring (0.47 a.u.).

In the series of compounds **VIII–XV** five π orbitals, one pseudo-π MO of X, one (compounds **XII–XIV**) or two (compounds **VIII–XI**) n_N MOs are observed. The first bands in the UPS spectra of **VIII–XV** are caused by single electron ionization processes from the π_5–X MO.

The sulfur and CH group substitution for nitrogen atoms in the five-membered ring (compounds **VIII–XI** and complexes **XII–XIV**) results in the destabilization of the HOMO energies by 0.3 eV. In compound **XIII**, the MO electronic levels of substituent R are higher than the respective levels in complex **X** by 0.8-1.2 eV. This is explained by the acceptor properties of the nitrogen atoms of the five-membered ring, which accept the electron density from the six-membered ring. As opposed to boron formazanates [34] and β-diketonates [27, 29, 31], there is no noticeable mixing of ligand π orbitals with the benzene ring MOs in complexes **IX–XI** and **XIII** (Table 2).

A noticeable mixing of orbitals of the chelate ligand and the $C_6H_{11}NH$ group was found for compounds **XIV–XV**. The presence of the nitrogen atom in the condensed ring (compound **XV**) causes the stabilization of the HOMO energy by 0.2 eV.

TABLE 2. Orbital Electron Energies (eV) and the Positions of Band Peaks from the Results of Gaussian Fitting of the Experimental Spectra (eV) of Compounds **VIII–XV**

Compound	MO	π_5–X	π_4–X*	n_N	π_3+X	X	R–X	R	n_N–X	n_N
VIII	$-\varepsilon_i$	6.18	7.17	7.44	–	–	–	–	–	–
	IE_i	7.99	9.24	9.53	–	–	–	–	–	–
IX	$-\varepsilon_i$	6.00	6.95	7.28	7.61	7.68	8.11	8.13	–	–
	IE_i	7.70	8.87	9.24	9.45	9.64	–	–	–	–
X	$-\varepsilon_i$	5.94	6.88	7.22	7.54	7.62	7.85	8.04	–	–
	IE_i	7.66	8.65	9.14	9.30	9.52	–	–	–	–
XI	$-\varepsilon_i$	6.00	6.97	7.28	7.59	7.67	7.74	8.00	–	–
	IE_i	7.74	8.74	9.06	9.32	9.48	9.63	–	–	–
XII	$-\varepsilon_i$	5.75	7.08	–	–	–	–	–	–	–
	IE_i	7.70	9.15	–	–	–	–	–	–	–
XIII	$-\varepsilon_i$	5.61	–	–	–	–	6.63; 7.19	7.17	–	–
	IE_i	7.50	–	–	–	–	8.61; 9.28	9.22	–	–
XIV	$-\varepsilon\varepsilon_i$	5.35	6.19	–	6.96	–	–	–	–	–
	IE_i	6.97	7.88	–	8.80	–	–	–	–	–
XV	$-\varepsilon_i$	5.56	6.30	–	–	–	–	–	6.99; 7.24	7.32
	IE_i	7.15	7.90	–	–	–	–	–	8.77; 9.01	9.22

* For compounds **XIV** and **XV** the energies of π_4–R and R–π_4 MOs are given.

Aza-boron-dipyridomethene derivatives. Below, the analysis of the UPS data and results of DFT calculations is reported for compounds **XVI–XVIII** [32].

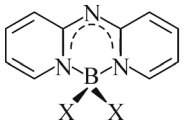

XVI X=C_2H_5
XVII X=C_3H_7
XVIII X=C_6H_5

Scheme 4. Compounds **XVI–XVIII**.

The optimization of the geometric parameters of complexes **XVI–XVII** in the starting symmetrical geometry (symmetry group C_2) gave the minimum energy when the alkyl groups are located on either side of the plane perpendicular to the chelate ring. The structure of compound **XVIII** corresponds to symmetry group C_{2v}, and the phenyl groups are arranged as in the β-diketonate analogue $(C_6H_5)_2$BAcac [30]. There are no marked differences in bond lengths and bond angles in the chelate rings in the series of the studied complexes.

The structures of **XVI–XVIII** have π systems isoelectronic with that of the anthracene molecule. In order to determine the effect of the complexing agent on the electronic structure of the complexes, we analyzed changes in the calculated electron energies and the orbital characters, passing from anthracene and acridine to the structure of **XVI** (Fig. 5). The anthracene, acridine, and **XVI** molecules are characterized by the presence of seven occupied π orbitals, and their HOMOs are localized on three rings. The field effect caused by the influence of two carbonyl carbon atoms (C2 and C4) in **XVI** stabilizes level n_N as compared to the respective value for the acridine molecule, which leads to an increase in the energy gap between the HOMO and HOMO-1 levels. The mixing of π orbitals of the chelate ligand and pseudo-π MOs of complexing agent X is observed for compounds **XVI–XVIII** (Table 3).

The propyl group substitution for ethyl groups (complex **XVII**) does not lead to noticeable changes in the energies and compositions of six higher occupied MOs. Under the effect of phenyl groups at the boron atom (complex **XVIII**) the MO levels of the chelate ligand are stabilized by 0.1-0.2 eV. The energy stabilization of the X–π level localized more on the BC_2 fragment is 0.7 eV.

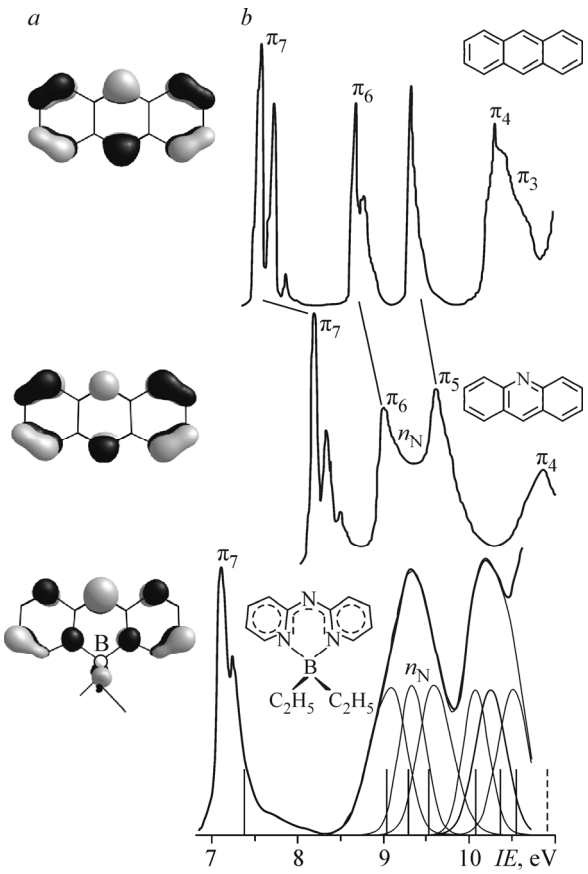

Fig. 5. Shapes of the HOMOs and photoelectron spectra of anthracene [54], acridine [55], and compound **XVI** [32] vapor (*a*). Based on the calculated data, the bands in the spectra of anthracene and acridine are compared (*b*).

TABLE 3. Orbital Electron Energies (eV) and the Positions of Band Peaks from the Results of Gaussian Fitting of the Experimental Spectra (eV) of Compounds **XVI–XVIII**

Compound	MO	π_7	X–π	X	n_N	π_6	X	π_5
XVI	$-\varepsilon_i$	5.31	6.98	–	7.23	7.47	8.02	8.30
	IE_i	7.11; 7.25	9.09	–	9.33	9.58	10.07	10.26
XVII	$-\varepsilon_i$	5.33	6.99	–	7.24	7.48	–	–
	IE_i	7.05; 7.25	8.87	–	9.24	9.49	–	–
XVIII	$-\varepsilon_i$	5.50	7.70	6.34-6.68	7.44	7.55	–	–
	IE_i	7.16; 7.34	9.83	8.47-8.88	9.45	9.56	–	–

In a series of compounds **XVI–XVIII** the fine structure of the first bands in the UPS spectra (Fig. 5, Table 3) is observed due to the C=C π_7 bonding HOMO localized on three rings, which is typical of of anthracene [54] and acridine [55] molecules.

Comparison of the experimental and calculated results for complexes IV–XVIII. In a series of compounds **IV–XVIII** experimental IEs and the calculated energies of electronic levels ε_i can be compared by shifting the energy scale by the average DFA defect for 70 electronic levels of all studied complexes, being 1.98 eV (Fig. 6*a*). However, if we average the DFA defect value δ_i separately for each complex and take into account the $\overline{\delta}_i$ dependence on the MO character, then the

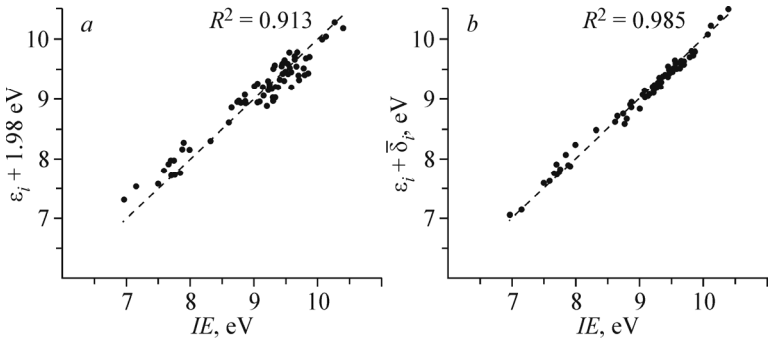

Fig. 6. Correlation between 70 calculated and experimental electron energies in 15 nitrogen-containing boron complexes.

average discrepancy between the experimental and theoretical IEs is 0.07 eV for 70 levels (Fig. 6*b*) at determination coefficient $R^2 = 0.985$. A similar procedure of comparing the UPS and DFT data was successfully applied in our review on boron β-diketonate complexes [26].

Therefore, within an accuracy of 0.1 eV, the calculated energies of the Kohn–Sham MOs reproduce the sequences of orbital IEs and the energy gaps between the electronic levels of nitrogen-containing boron complexes.

CONCLUSIONS

Our researches revealed that in the series of nitrogen-containing boron complexes (β-diketonates, imidoylamidinates, and formazanates) the HOMO was of the same nature and the HOMO-1 orbital of nitrogen-containing molecules was determined by the presence of lone pairs of nitrogen atoms. There is no noticeable mixing of π orbitals of the chelate ring and the aromatic substituents in imidoylamidinate complexes, typical of boron β-diketonates and formazanates. The presence of nitrogen atoms in the condensed ring stabilizes the HOMO electron energies by 0.2-0.3 eV and π orbital electrons energies in the benzene ring by 0.8-1.2 eV. The HOMOs of three substituted aza-boron-dipyridomethene correlate with the π_7 orbital of anthracene and acridine, hence, their UPS spectra have a fine structure of the first band. The quantum chemical DFT approximation (B3LYP functional and TZVPP basis set) is optimal to calculate the electronic structure and interpret the UPS spectra of nitrogen-containing boron complexes.

The work was supported by the Ministry of Education and Science of the RF (State Task, Project 16.5904.2017/BCh).

REFERENCES

1. S. Chibani, A. Charaf-Eddin, B. Mennucci, et al., *J. Chem. Theory Comput.*, **10**, 805-815 (2014).
2. Y. Pi, D.-J. Wang, H. Liu, et al., *Spectrochim. Acta, A*, **131**, 209 (2014).
3. A. D′Al o, V. Heresanu, M. Giorgi, et al., *J. Phys. Chem. C*, **118**, 1906 (2014).
4. C. Qian, G. Hong, M. Liu, P. Xue, and R. Lu, *Tetrahedron*, **70**, 3935 (2014).
5. W. A. Morris, T. Liu, and C. L. Fraser, *J. Mater. Chem. C*, **3**, 352 (2015).
6. M. J. Mayoral, P. Ovejero, M. Cano, and G. Orellana, *Dalton Trans.*, **40**, 377 (2011).
7. I. Sánchez, J. A. Campo, J. V. Heras, et al., *Inorg. Chim. Acta*, **381**, 124 (2012).
8. E. Giziroglu, A. Nesrullajev, and N. Orhan, *J. Mol. Struct.*, **1057**, 246 (2014).
9. A. Flores-Parra and R. Contreras, *Coord. Chem. Rev.*, **196**, 85 (2000).
10. P. Czerney, G. Haucke, and C. Igney, *Ger (East) DD/-265266*, CA, **112**, No. 45278 (1990).
11. M. Halik, G. Schmid, and L. Davis, *German patent 10152938*, CA, **123**, No. 378622 (2003).
12. R. Kammler, G. Bourhill, Y. Jin, et al., *J. Chem. Soc., Faraday Trans.*, **92**, 945 (1996).

13. K. Tanaka, K. Tamashima, A. Nagai, et al., *Macromole.*, **46**, 2969 (2013).
14. G. Zhang, R. E. Evans, K. A. Campbell, and C. L. Fraser, *Macromole.*, **42**, 8627 (2009).
15. J. Banuelos, F. L. Arbeloa, V. Martinez, et al., *Phys. Chem. Chem. Phys.*, **13**, 3437 (2011).
16. Y. Deng, Y.-Y. Cheng, H. Liu, et al., *Tetrahedron Lett.*, **55**, 3792 (2014).
17. S. M. Barbon, V. N. Staroverov, and J. B. Gilroy, *J. Org. Chem.*, **80**, 5226 (2015).
18. M. Hesari, S. M. Barbon, V. N. Staroverov, et al., *Chem. Commun.*, **51**, 3766 (2015).
19. R. R. Maar, S. M. Barbon, N. Sharma, et al., *Chem. Eur. J.*, **21**, 15589 (2015).
20. D. Wang, R. Liu, C. Chen, et al., *Dyes Pigm.*, **99**, 240 (2013).
21. J. H. Gibbs, H. Wang, D. K. Bhupathiraju, et al., *J. Organomet. Chem.*, **798**, 209 (2015).
22. S. P. Singh and T. Gayathri, *Eur. J. Org. Chem.*, **22**, 4689 (2014).
23. T. Papalia, G. Siracusano, I. Colao, et al., *Dyes Pigm.*, **110**, 67 (2014).
24. D. Gong, Y. Tian, C. Yang, et al., *Biosens. Bioelectron.*, **85**, 178 (2016).
25. S. Hüfner, *Photoelectron Spectroscopy: Principles and Applications*, Springer, Berlin (1996).
26. I. S. Osmushko, V. I. Vovna, S. A. Tikhonov, et al., *Int. J. Quantum Chem.*, **116**, 325 (2016).
27. V. I. Vovna, S. A. Tikhonov, and I. B. Lvov, *Russ. J. Phys. Chem. A*, **85**, 1942 (2011).
28. V. I. Vovna, S. A. Tikhonov, and I. B. Lvov, *Russ. J. Phys. Chem. A*, **87**, 688 (2013).
29. V. I. Vovna, S. A. Tikhonov, M. V. Kazachek, et al., *J. Electron. Spectrosc. Relat. Phenom.*, **189**, 116 (2013).
30. S. A. Tikhonov, I. B. Lvov, and V. I. Vovna, *Rus. J. Phys. Chem. B*, **8**, 626 (2014).
31. V. I. Vovna, S. A. Tikhonov, I. B. Lvov, et al., *J. Electron. Spectrosc. Relat. Phenom.*, **197**, 43 (2014).
32. S. A. Tikhonov and V. I. Vovna, *J. Struct. Chem.*, **56**, No. 3, 446-453 (2015).
33. S. A. Tikhonov, V. I. Vovna, and A. V. Borisenko, *J. Mol. Struct.*, **1115**, 1 (2016).
34. S. A. Tikhonov, V. I. Vovna, and A. V. Borisenko, *J. Electron Spectrosc. Relat. Phenom.*, **213**, 32 (2016).
35. B. M. Mikhailov, V. A. Dorokhov, and V. I. Seredenko, *Bull. Acad. Sci. USSR Div. Chem. Sci.*, **27**, 1205 (1978).
36. V. A. Dorokhov, L. I. Lavrinovich, A. S. Shashkov, and B. M. Mikhailov, *Bull. Acad. Sci. USSR Div. Chem. Sci.*, **30**, 1097 (1981).
37. V. A. Dorokhov, A. R. Amamchyan, M. N. Bochkareva, et al., *Bull. Acad. Sci. USSR Div. Chem. Sci.*, **36**, 147 (1987).
38. E. K. U. Gross, E. Runge, and O. Heinonen, *Many Particle Theory*, Adam Hilger (1992).
39. E. N. Economou, *Green's Functions in Quantum Physics*, Springer, New York (1979).
40. S. Hamel, P. Duffy, M. E. Casida, and D. R. Salahub, *J. Electron. Spectrosc. Relat. Phenom.*, **123**, 345 (2002).
41. P. Duffy, D. P. Chong, M. E. Casida, and D. R. Salagub, *Phys. Rev. A*, **50**, 4707 (1994).
42. A. A. Granovsky; http://classic.chem.msu.su/gran/firefly/index.html.
43. *Basis Set Exchange*, Version 1.2.2: https://bse.pnl.gov/bse/portal.
44. K. Eichkorn, F. Weigend, O. Treutler, and R. Ahlrichs, *Theor. Chem. Acc.*, **119**, 97 (1997).
45. M. V. Kazachek and I. V. Svistunova, *Spectrochim. Acta A*, **148**, 60 (2015).
46. Y. Kubota, K. Kasatani, H. Takai, et al., *Dalton Trans.*, **44**, 3326 (2015).
47. M.-C. Chang and E. Otten, *Inorg. Chem.*, **54**, 8656 (2015).
48. S. A. Tikhonov, V. I. Vovna, N. A. Gelfand, et al., *J. Phys. Chem. A*, **120**, 7361 (2016).
49. C. Lee, W. Yang, and R. G. Parr, *Phys. Rev. B: Condens. Matter Mater. Phys.*, **37**, 785 (1988).
50. A. D. Becke, *J. Chem. Phys.*, **98**, 5648 (1993).
51. P. J. Stephens, F. J. Devlin, C. F. Chabalowski, et al., *J. Phys. Chem.*, **98**, 11623 (1994).
52. L. Asbrink, O. Edqvist, E. Lindholm, and L. E. Selin, *Chem. Phys. Let.*, **5**, 192 (1970).
53. W. V. Niessen, W. P. Kraemer, and G. H. F. Diercksen, *Chem. Phys.*, **41**, 113 (1979).
54. T. Kajiwara, S. Masuda, K. Ohno, and Y. Harada, *J. Chem. Soc. Perkin II*, **4**, 507 (1988).
55. J. P. Maier and J.-F. Muller, *Helv. Chim. Acta*, **58**, 1641 (1975).